Computers & Geosciences 90 (2016) 57–65

Contents lists available at ScienceDirect

Computers & Geosciences

journal homepage: www.elsevier.com/locate/cageo

Case study

Sensitivity of a third generation wave model to wind and boundary condition sources and model physics: A case study from the South Atlantic Ocean off Brazil coast

S. Mostafa Siadatmousavi [a], Felix Jose [b,*], Graziela Miot da Silva [c]

[a] Department of Civil Engineering, Iran University of Science and Technology, Narmak, 1684613114, Tehran, Iran
[b] Department of Marine and Ecological Sciences, Florida Gulf Coast University, Fort Myers, FL 33965-6565, United States of America
[c] School of the Environment, Flinders University, GPO Box 2100, Adelaide, SA 5001, Australia

ARTICLE INFO

Article history:
Received 24 December 2014
Received in revised form
25 September 2015
Accepted 30 September 2015
Available online 3 October 2015

Keywords:
White capping
Wave spectrum
Model uncertainties
Santa Catarina Island

ABSTRACT

Three different packages describing the white capping dissipation process, and the corresponding energy input from wind to wave were used to study the surface wave dynamics in South Atlantic Ocean, close to the Brazilian coast. A host of statistical parameters were computed to evaluate the performance of wave model in terms of simulated bulk wave parameters. Wave measurements from a buoy deployed off Santa Catarina Island, Southern Brazil and data along the tracks of Synthetic Aperture Radars were compared with simulated bulk wave parameters; especially significant wave height, for skill assessment of different packages. It has been shown that using a single parameter representing the performance of source and sink terms in the wave model, or relying on data from only one period of simulations for model validation and skill assessment would be misleading. The model sensitivity to input parameters such as time step and grid size were addressed using multiple datasets. The wind data used for the simulation were obtained from two different sources, and provided the opportunity to evaluate the importance of input data quality. The wind speed extracted from remote sensing satellites was compared to wind datasets used for wave modeling. The simulation results showed that the wind quality and its spatial resolution is highly correlated to the quality of model output. Two different sources of wave information along the open boundaries of the model domain were used for skill assessment of a high resolution wave model for the study area. It has been shown, based on the sensitivity analysis, that the effect of using different boundary conditions would decrease as the distance from the open boundary increases; however, the difference were still noticeable at the buoy location which was located 200–300 km away from the model boundaries; but restricted to the narrow band of the low frequency wave spectrum.

1. Introduction

All third generation wave models are based on the wave action balance equation to simulate the directional wave spectrum. In these models, the wave spectrum at each time step is determined according to the following equation:

$$\frac{DN}{Dt} \equiv \frac{S}{\sigma} \tag{1}$$

in which D/Dt represents the total time derivative (includes local rate, as well as spatial and spectral derivatives), and Srepresents all energy sources and sinks terms. The energy transfer from wind to the waves, quadruplet nonlinear wave interaction, and white capping dissipation are the three main mechanisms controlling the wave growth and decay in deep waters. Among these three source/sink mechanisms, the white capping dissipation is the least understood term, and several formulations have been proposed to include it in a more realistic form in the third generation wave models (Cavaleri et al., 2007).

In this study, an unstructured flexible mesh was employed to study the surface wave dynamics in the South Atlantic Ocean close to the Brazilian coast, during several months in 2002 and 2003. The uncertainties in model forecasts and its sensitivity to the formulations used for simulating the physics associated with white capping were addressed by comparing the model outputs, especially significant wave height, using different model configurations with *in situ* measurements from an offshore buoy location. Moreover, significant wave height and wind speed measurements from satellite altimeters were employed for validation of model inputs and outputs.

* Corresponding author.
E-mail addresses: siadatmousavi@iust.ac.ir (S.M. Siadatmousavi), fjose@fgcu.edu (F. Jose).

http://dx.doi.org/10.1016/j.cageo.2015.09.025
0098-3004/

2. Method

2.1. Study area and model setup

The wave hindcasting using different parameterization for white capping and wind input terms were performed for South Atlantic Ocean off the coast of Brazil (see Fig. 1). The unstructured computational grid, covering the south-central Brazil coast and offshore, was produced using SMS software (Aquaveo, 2010), and the required bathymetry data were obtained from Nautical Charts of Brazilian Department of Hydrography and Navigation (DHN). The flexible mesh grid composed of 8608 triangles and 4481 vertices, with mesh element size varied from approximately 10 km along the deep water open boundaries, which was located mostly beyond the continental shelf, to less than 2 km close to the buoy location (off the Santa Catarina Island, see Fig. 1) and in shallow waters.

The third generation wave model SWAN (Simulating Waves Nearshore), version 41.01 was used for wave modeling (SWAN TEAM, 2014). Simulations were performed with full spectral formulation using frequency band ranging from 0.039 to 0.619 Hz, and 36 directional bins. Linear wave growth, in response to wind forcing, was activated using formulations proposed by (Cavaleri and Rizzoli, 1981). Exponential wave growth and white capping terms were computed from three different packages: WAM Cycle 3 (denoted by KOM hereafter), WAM Cycle 4 (denoted by JAN hereafter) and the formulation presented by (van der Westhuysen et al., 2007) (denoted by WST hereafter). KOM formulation employs the pulse-based quasi-linear model of (Hasselmann, 1974) for white capping term, and a rescaled version of energy transfer from wind to wave as proposed by (Snyder et al., 1981). In order to accommodate the underestimation of wave period by KOM formulation, (Rogers et al., 2003) suggested to use a second order dependence of white capping dissipation on wavenumber; instead of linear relationship as earlier suggested by (Hasselmann, 1974). This modification became part of SWAN model suite since version 41.01.

In JAN formulation, two-way interaction of wave and wind were taken into account in wind term, using formulation presented by (Janssen, 1991). Moreover, a combination of linear and quadratic terms are used to realistically include the wave dissipation by white capping process in high frequency end of the spectrum. Both WAM formulations (KOM and JAN) suffer from erroneous over-prediction of wind-sea (chops) in the presence of swell waves because of the dependence of dissipation term on mean wavenumber and wave steepness (Ardhuin et al., 2010; Young and Babanin, 2006). In WST formulation, a nonlinear saturated-base white capping equation is presented to solve this over-prediction problem (van der Westhuysen et al., 2007). Also, the wind input term from (Yan, 1987) was used, instead of the formulation presented by (Snyder et al., 1981), to improve the results during high wind speed events.

It is worth to note that in version 41.01, SWAN employs updated coefficients for frequency tail of power spectrum compared to the original formulations presented in (Komen et al., 1984); which is critical in defining nonlinear interaction term, and have impacts on wave growth. Moreover, new drag coefficient formulation was used in wind input term to avoid unrealistically large values for drag coefficient associated with high wind velocities (SWAN TEAM, 2014).

In all simulations presented in this study, the Discrete Interaction Approximation (DIA) method was employed for quadruplet wave-wave interaction term, due to its computational efficiency (Hasselmann and Hasselmann, 1985). Shallow water terms such as triad wave–wave interaction and the spectral form of the bore model for depth-induced wave breaking were also included in the computations (Eldeberky, 1997). We would not expect any influence from these latter terms, which were meant for wave transformations in shallow water, on the model data presented here because all the measurements used for model skill-assessments were in deep water. The empirical formulation of JONSWAP (Hasselmann et al., 1973) was included in the model setup to take into account wave dissipation due to bottom friction. The constant value of 0.038 $m^2 s^{-3}$ was used as bottom friction coefficient for entire study area, as suggested by (Zijlema et al., 2012)

Note that Eq. (1) is solved on discrete frequencies in SWAN, and therefore the minimum and maximum frequencies used in the computations needs to be set by the user. Due to the shape of normal wind-induced wave spectrum, not much energy is retained in frequencies lower than 0.05 Hz (wave period of 20 s). Therefore, the minimum frequency is usually set within the range of 0.03–0.05 Hz (Janssen, 2008). On the other hand, the wave energy decays slowly in high frequency part of the spectrum. SWAN Team recommended 1 Hz for high frequency cut-off but (Siadatmousavi et al., 2012) showed that the modeling would be more successful in reproducing the wave spectrum and bulk wave parameters in oceanic scales if the high frequency cut-off were set to some values close to 0.5 Hz, as used in other deep water wave models (Janssen, 2008). Therefore the value of 0.6 Hz was used for high frequency cut-off in this study.

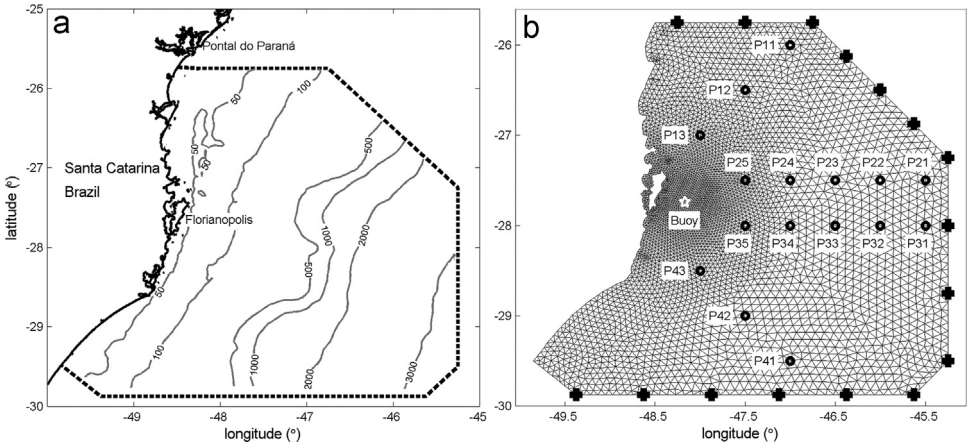

Fig. 1. (a) The study area and (b) the unstructured mesh used for simulations. The gray contours are isobaths. The locations of provided open boundary data marked by the black plus marks, and the location of buoy used for verification of the models was shown by a white pentagram mark. The wave spectrum at points $_{Pi}$ were used to assess the model sensitivity to the boundary conditions.

2.2. Input data

In order to evaluate the model sensitivity to the quality of the wind data, two wind datasets were used for this study: (i) GROW-Fine SAM wind data from Oceanweather Inc. which had a temporal resolution of 3 h and spatial resolution of 0.125° and (ii): ECMWF ERA-Interim dataset which provided temporal resolution of 6 h, and spatial resolution of 0.125°. As shown in Fig. 1, the southern open boundary of the model extended from 45° to 50° West (~500 km) along the 30° South latitude. The Continental shelf is very narrow in this region, compared to the shelf farther north. The open northern boundary extended from 46.5° to 48.5° west (~218 km). This northern boundary was located entirely on the continental shelf off Pontal do Paraná (Fig. 1a). The eastern open boundary was mostly in deep water, and hence a coarser (~10 km) spatial resolution was chosen for the computational grid along this boundary. The directional wave spectra from GROW-Fine simulations (Ocean weather Inc.) were available for the months of March and May in 2002 as well as for August and September in 2003. The time series of model wave data for the four months were extracted for the locations marked by thick plus sign in Fig. 1. Another open boundary wave dataset was extracted from a global WAVEWATCH-III wave model (Tolman, 2002). Simulations were performed for entire earth with grid sizes of 1.25° in longitudinal direction and 1.00 degree in latitude direction. The model setup, as well as required input data were downloaded from NOAA webpage (http://polar.ncep.noaa.gov/waves/download.shtml?). The outstanding performance of WAVEWATCH-III wave model for large scale oceanic simulations were reported before (Hanson et al., 2009), it can be therefore used as a valuable source to provide boundary conditions of high resolution spectral wave data for the given regional study.

The hourly bulk wave parameters such as significant wave height (H_s) and peak wave period (T_p) were measured using a directional waverider buoy (Datawell Waverider Mark II), deployed at a water depth of approximately 80 m, at approximately 35 km offshore Santa Catarina Island in Southern Brazil (Fig. 1b). The buoy was deployed and maintained by Marine Hydraulics Laboratory (LAHIMAR) of the Federal University of Santa Catarina (UFSC). The buoy data were used for model skill assessment, using different model configurations.

Synthetic Aperture Radar (SAR) images also provided another valuable data source, available in the public domain, for validation of simulated wind and wave data. The final SAR products from eight satellites were downloaded for time periods corresponding to this study, from GlobWave dataset via ftp server of French Research Institute for Exploitation of the Sea (ftp://ftp.ifremer.fr/ifremer/cersat/products/swath/altimeters/waves/data).

2.3. Skill assessment indices

In order to evaluate the agreement between two time series data sets, (e.g. model prediction and *in situ* observations), the following statistical parameters were used (Willmott, 1982):

Bias:

$$\text{Bias} = N^{-1}\sum_{i=1}^{N}(M_i - O_i) \tag{2}$$

Root mean square error (also called root mean square difference (RMSD) if it is calculated for two time series of model outputs):

$$\text{RMSE} = \sqrt{N^{-1}\sum_{i=1}^{N}(O_i - M_i)^2} \tag{3}$$

Correlation coefficient:

$$r = \frac{N\sum_{i=1}^{N}O_iM_i - \left(\sum_{i=1}^{N}M_i\right)\left(\sum_{i=1}^{N}O_i\right)}{\sqrt{N\left(\sum_{i=1}^{N}O_i^2\right) - \left(\sum_{i=1}^{N}O_i\right)^2}\sqrt{N\left(\sum_{i=1}^{N}M_i^2\right) - \left(\sum_{i=1}^{N}M_i\right)^2}} \tag{4}$$

Index of agreement:

$$d = 1 - \frac{\sum_{i=1}^{N}(M_i - O_i)^2}{\sum_{i=1}^{N}\left(|M'_i| + |O'_i|\right)^2} \tag{5}$$

in which O_i and M_i denote ith data from observation and model respectively, $|M'_i|$ and $|O'_i|$ are deviations from the mean values of observations and model results, and N is the total number of data points.

The inclusion of multiple statistical indices is necessary to avoid pitfalls associated with using a single parameter. For example, the bias compares the mean of two time series and therefore explains the systematic error between two time series but does not include any information about the distribution of data around the mean value. The correlation coefficient describes a linear relationship between two variables but does not indicate exact equality of two variables. Root mean square error explains the scatter of model results around the observations, but it is not bounded and therefore it is not easy to decide when it is small-enough.

3. Results and discussion

3.1. Uncertainties in wind input

For the ease of evaluating the model uncertainties using three different parameterizations, a series of reference stations were established within the model domain and they were named P11–P41 (see Fig. 1). The model comparison using KOM, JAN and WST formulations were conducted for these reference stations. Two parallel transects were identified north and south of the buoy location with equidistant points selected from deep water into the inner continental shelf.

Performance of a wave model is critically dependent on the quality and spatial resolution of wind data used (Kumar et al., 2000; Siadatmousavi et al., 2009). Therefore it is pertinent to evaluate the quality of the two diverse wind datasets used for simulations. The temporal resolution of ECMWF data was 6 h while GROW-Fine SAM wind data had a time interval of 3 h. All comparisons in this section were reported based on a temporal resolution of 6 h so that both datasets had data. Since most of the measurements for validation tests were available only from deep water, wind data from the coast and within 30 km from coastlines were removed from all datasets before calculating the statistical parameters. The wind speed from two datasets was also expected to diverge close to the land due to uncertainties in modeling the frictional effect of land on wind. Since these differences have minor effects on simulated wave data from offshore water, it is better to remove those wind data before comparing the datasets. This discrepancy of dataset close to the coastline was shown in Fig. 2a in which spatial distribution of bias for the two wind dataset was plotted for March 2002. It is evident that most of differences (~2 m/s) occurred close to the coastline.

The mean and maximum wind speed at reference station P34 (shown in Fig. 1b) for all time periods considered in this study are presented in Table 1. The maximum and mean wind velocities from both wind dataset show that the weather conditions were more severe during August–September (southern hemisphere winter) than March and May (summer). Moreover the wind speed from Grow-Fine dataset was higher than from ECMWF data. The

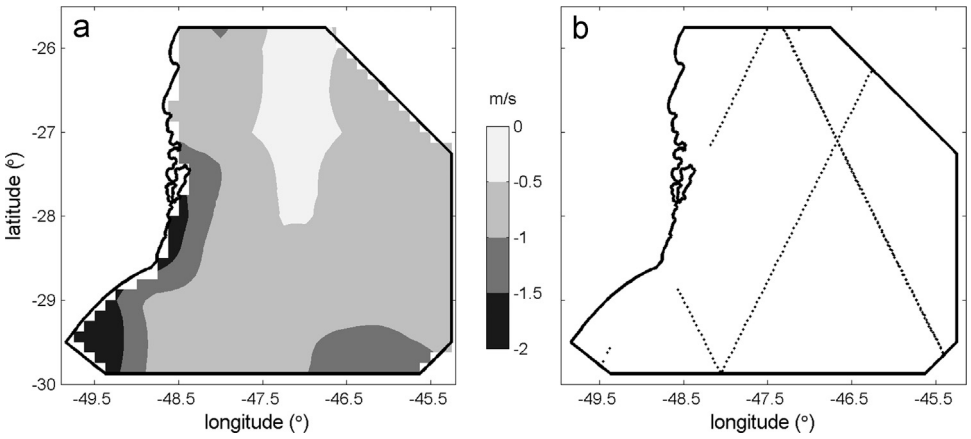

Fig. 2. (a) The difference of temporal mean of two wind dataset for March 2002 and (b) the SAR tracks over study area during March 2002 (The points close to the coastline were removed).

maximum bias (7.5 − 6.4 = 1.1 m/s) and RMSD (2.2 m/s) occurred for May 2002. The minimum correlation coefficient also occurred for this time period. Therefore it is expected that simulated wave data using different wind input would differ significantly for May 2002, as confirmed by subsequent SWAN model runs (results not shown).

In order to validate the input wind datasets, both time series were compared with wind speed derived from SAR data. To do a meaningful comparison, only the satellite cycles within 30 min of model winds were considered and the data from the closest grid to satellite track were used. Moreover, parts of tracks close to the coastline were neglected from the analysis, based on the reason described earlier. The number of available data for comparisons as well as statistical parameters describing the quality of data from two sources are presented in Table 2, and the corresponding tracks for March 2002 are shown in Fig. 2b. During March 2002 the computed statistics were not conclusive. The Grow-Fine data had better Bias than ECMWF data so the mean value of wind speed was better predicted by Grow-Fine data. However, the correlation coefficient and index of agreements showed that ECMWF variations were in better agreement with satellite data. On the other hand, In May 2002 all statistics shows the superiority of Grow-Fine data when compared with ECMWF. In 2003 time period, both wind data were in good agreement with satellite measurements but Grow-Fine data had slightly better statistics than ECMWF. Therefore it is expected to have better results of wave simulations during May 2002 and August–September 2003 periods using Grow-Fine data.

3.2. Uncertainties in wave boundary conditions

The directional wave spectrum used as boundary conditions from Grow-Fine data and WAVEWATCH-III had some fundamental differences. The spectrum evolutions from both sources at a boundary point near to P31 reference station is presented in Fig. 3a and b. The difference between the two spectrum evolutions is presented in Fig. 3c in which red (blue) colors means higher (lower) energy level in Grow-Fine data than WAVEWATCH-III data. A significant contrast between two data source was higher level of wave energy in frequencies lower than 0.1 Hz in WAVEWATCH-III data (shown in Fig. 3b), e.g. during May 17–20 and May 6–7 periods. On the other hand, the energy level in the band of 0.1–0.3 Hz was in general higher in Grow-fine wave spectra, e.g. during May 3, 7, 15–17, 18–19 and 22 and 27 periods (Fig. 3c). Although not easy to see in Fig. 3, slightly higher level of energy existed in frequencies higher than 0.3 Hz in WAVEWATCH-III spectrum than corresponding Grow-Fine data.

The discrepancy between two dataset came from the fact that Grow-fine simulations were performed using a modified WAM formulations for global simulations. However, WAVEWATCH-III employed a combination of a low frequency dissipation term similar to energy dissipation by turbulence mechanism, and an empirical high frequency dissipation term (Tolman and Chalikov, 1996). Such dissipation could effectively distinguish between dynamics of sea and swell, while WAM formulations suffer from over-estimation of sea waves and under-estimation of swell waves (Ardhuin et al., 2010). The reported better performance of WAVEWATCH-III wave model compared to other models when used for large scale domains with complex sea states (Hanson et al., 2009) might be related to this feature.

In order to investigate the dynamics of sea and swells in two datasets, the integral separation algorithm of (Hwang et al., 2012) was used to separate wind sea and swell components of 3-hourly wave spectra in May 2002 For each part of sea and swell, the wave height were calculated and the results were presented in Fig. 4. It is evident that swell wave height in WAVEWATCH-III data were almost 0.5 m higher than corresponding values in Grow-Fine data during entire May 2002 ($bias_{WW3,swell} - bias_{GrowF,swell} = 0.46$ m). The wind sea height were close to each other for both models, but Grow-Fine data contains slightly more energy in sea waves than

Table 1
The maximum and mean values of wind speed from ECMWF and GROW-Fine dataset during different time periods for point P34. The correlation coefficient (r) and root mean square difference between two time series during each time period were also shown.

Time period	March 2002		May 2002		Aug–Sep 2003	
Parameter	ECMWF	GROW-Fine	ECMWF	GROW-Fine	ECMWF	GROW-Fine
Maximum U10 (m/s)	12.4	13.5	13.9	17.7	14.9	18.5
Average (m/s)	5.5	6.0	6.4	7.5	7.1	8.0
r	0.75		0.71		0.85	
RMSD (m/s)	1.8		2.2		1.8	

Table 2
Comparison of wind sources with satellite data.

Time period	March 2002		May 2002		Aug–Sep 2003	
Parameter	ECMWF	GROW-Fine	ECMWF	GROW-Fine	ECMWF	GROW-Fine
Bias	−1.1	−0.3	−4.7	−0.9	−1.0	0.1
RMSE (m/s)	1.4	1.4	6.4	2.3	2.0	1.7
r	0.85	0.6	0.26	0.9	0.92	0.92
d	0.79	0.72	0.05	0.91	0.95	0.96
Number of available data for comparisons	270		217		358	

WAVEWATCH-III for most of the time ($bias_{WW3,sea} - bias_{GrowF,sea} = -0.06$ m).

Furthermore, WAVEWATCH-III uses the wind input term based on the formulation of (Chalikov, 1995). This formulation takes into account energy transfer from waves to wind when wave travels faster than wind, or in opposing wind condition. Therefore another potential source for the difference between outputs from two wave models are the wind input terms used in WAVEWATCH-III and Grow-Fine simulations.

The root mean square difference for the two time series of significant wave height, calculated from SWAN using different boundary conditions are presented in Fig. 5, for several reference staions within the model domain (see Fig. 1b). Both simulations were performed using Grow-Fine wind data, and using JAN formulation for white capping and wind input formulations. Along the two east–west transects, the middle blocks in Fig. 5, the RMSD progressively decreases as the waves propagate farther away from the domain boundary. Same trend can be noticed for the northern and southern transects also. It is evident that importance of the uncertainty in wave boundary conditions decreases as the distance from the boundary increases. However, the difference is still not negligible close to the buoy location near to the coast. The same results were obtained using KOM and JAN formulations also (not shown).

3.3. Model sensitivity to the source terms

Three different packages were available for computing the energy transfer from wind to waves, and white capping energy dissipations. The calibration parameters within these formulations were set such that the model could reproduce wave spectrum in fully developed conditions (Komen et al., 1984, 1996; Rogers et al., 2003; van der Westhuysen et al., 2007). Such generalized coefficients might not be the optimum values for specific study area and for varying wind and wave climate (Siadatmousavi et al., 2011). However, no efforts were made in this study to tune the coefficients within these formulations, and instead, all formulations were used using original values presented in the model. Our objective was to compare these formulations in terms of model performance and thereby evaluating the model efficiency in reproducing the measured bulk wave parameters.

The quadratic nonlinear wave–wave interaction was incorporated in the computations using Discrete Interaction Approximation (DIA), as otherwise, intense computational resources were needed to use the full formulation of nonlinear interaction (Hasselmann et al., 1985; van Vledder, 2006). Although DIA method has some inherent deficiency in reproducing the wave spectrum (van Vledder, 2006), it is quite successful in reproducing bulk wave parameters (Komen et al., 1996), which will be used in this study for skill assessment of the model.

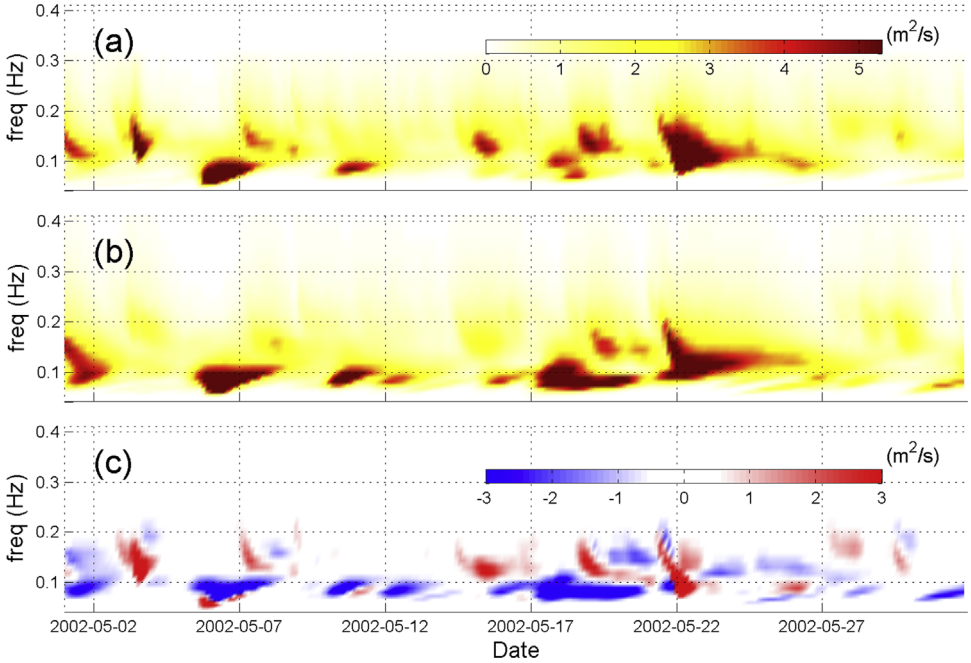

Fig. 3. Spectral evolution for May 2002 at the closest boundary to the point P31 shown in Fig. 1 using (a) Grow-fine wave data; (b) WAVEWATCH-III global simulation. (c): the difference between spectral evolution shown in panels (a) and (b). (For interpretation of the references to color in this figure, the reader is referred to the web version of this article.).

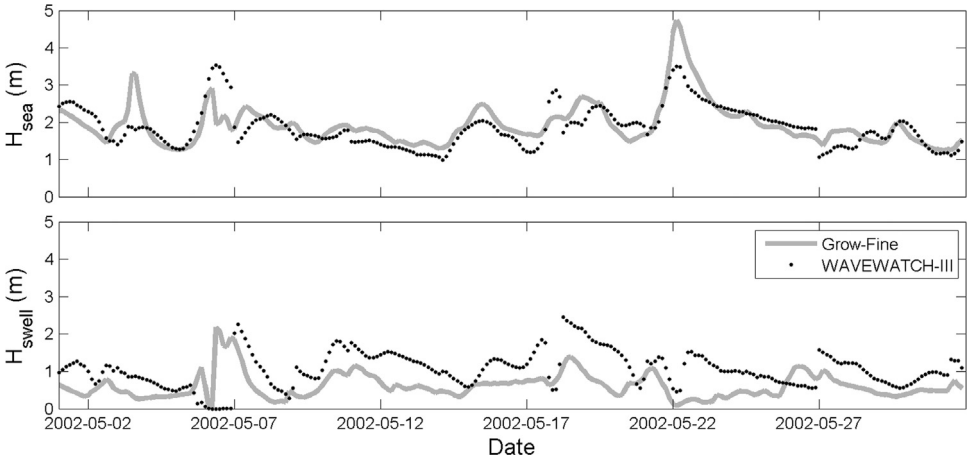

Fig. 4. Time series of (a) wind sea and (b) swell for May 2002 at the closest boundary to the point P31 shown in Fig. 1 using (a) Grow-fine wave data and (b) WAVEWATCH-III global simulation.

3.4. Sensitivity to grid size and time step

The spatial resolution used in the unstructured mesh (Fig. 1b) is acceptable for wave modeling for the offshore and inner shelf environments (Cavaleri et al., 2007). However, another computational mesh with almost double the resolution was generated using SMS and few simulations were repeated to ensure the adequacy of the chosen spatial resolution. The variation in the significant wave height time series generated for the offshore buoy location from SWAN runs using different mesh files did not exceeded 2 cm (less than 1%) in all simulations. Therefore the spatial resolution of the computational mesh used in this study would not affect the conclusions.

SWAN uses implicit scheme to solve wave action equation and therefore the user-specified time step only affects the accuracy of the simulation and not the numerical stability. In all simulations, a time step of 10 min was used for numerical solutions. However, in order to ensure that time step selection would not affect the model outputs, few simulations were repeated using time step of 5 min. The change in significant wave height at buoy location with this reduced time step was limited to less than 1 cm (less than 1%). Therefore the selected time step was small enough for time integration of wave action equation.

A personal computer with Intel® core™ i7-3370 processor was used for all simulations. The computational time scaled almost linearly with the number of cores employed. Using the time step of 10 min and the computational grid shown in Fig. 1b, the simulations for all 4 month in 2002 and 2003 using KOM, WST and JAN formulations took 3106, 3271 and 4494 s respectively, when 8 cores were used.

3.5. Comparison with Buoy data

The time series of significant wave height measured at buoy location along with SWAN results using KOM and WST formulations for August–September 2003 are presented in Fig. 6a. In this batch of simulations wind data and wave boundary conditions from Grow-Fine datasets were used. In general KOM formulation resulted in higher wave heights than WST formulation. Several periods of over-predictions (e.g. August 3–6, September 19–21) and under-prediction (e.g. August 26, September 10) occurred in both SWAN results. The predicted peak wave period from model using KOM and WST formulations were compared to buoy data in Fig. 6b. The results from both formulation were basically the same except for a few hours on August 10 and September 25 in which KOM predicted slightly higher wave period than WST. Both formulation were in moderate agreement with buoy data. During low energy condition such as on August 3 or September 20, both formulation underestimated the peak period.

A detailed statistical comparison of predicted wave height using KOM, JAN and WST methods for three separate periods of simulations during 2002 and 2003 are presented in Table 3. Note that the bias of significant wave height was positive for all method and the bias of the peak wave period was negative in all configurations. In general, the best statistics were obtained using WST formulations. The difference between performance statistics of KOM and JAN formations were small, and KOM formulations resulted in slightly better results.

As mentioned in Section 3.1, ECMWF wind speeds were generally lower than Grow-Fine wind speeds. Therefore it is not surprising that the significant wave height from SWAN using ECMWF become lower than SWAN results using Grow-Fine wind speeds. For example the bias and RMSE using WST formulation were 0.09 and 0.37 m for time period of August–September 2003, as

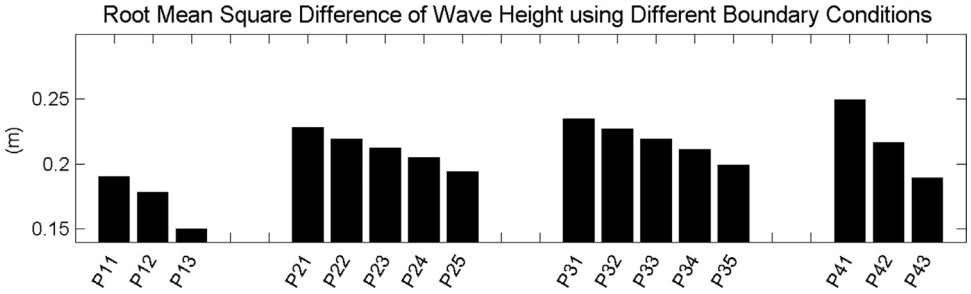

Fig. 5. The root mean square difference of two time series of significant wave height calculated from SWAN using two different boundary conditions.

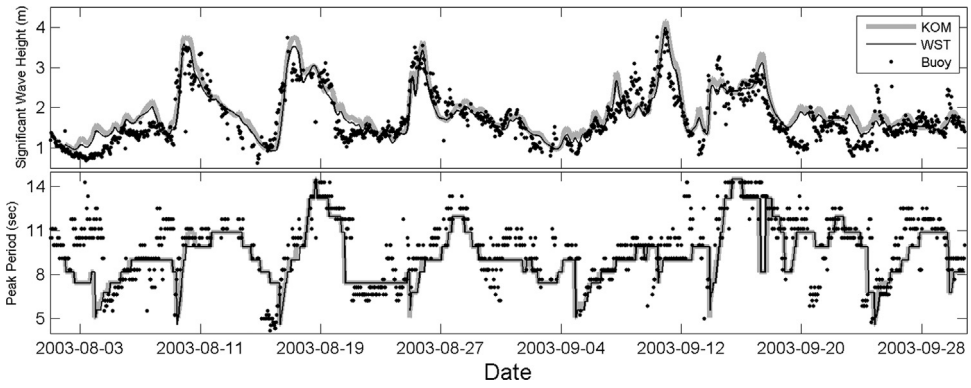

Fig. 6. Time series of (a) significant wave height; (b) peak wave period at buoy location from SWAN results using KOM formulation (gray thick line), using WST formulation (black thin line) and from Buoy measurements (dots).

presented in Table 3. When ECMWF wind was used in the simulations, the bias and RMSE became −0.06 and 0.41 m. Moreover the *r* and *d* indices were 0.79 and 0.85, respectively using ECMWF, which were lower than their corresponding values obtained using Grow-Fine wind data (0.84 and 0.91 for *r* and *d*, respectively). The lower bias resulted from the lower ECMWF wind speed values and higher RMSE indicates the lower quality of wind speed during this time period when compared with Grow-fine wind data. Note that in terms of absolute value, the bias was improved using ECMWF but when other statistical parameters such as RMSE, *r* and *d* were considered, it is possible to decide which wind data resulted in more accurate wave results.

Two different boundary conditions available for wave simulations were described in Section 3.2. Using wave spectrum from global WAVEWATCH-III simulations, as boundary conditions, decreased the performance of SWAN using WST formulation at buoy location. The bias and RMSE became 0.16 and 0.43 m, and non-dimensional indices, *r* and *d*, became 0.8 and 0.87, respectively. Inspection of spectrum evolutions from two simulations showed that the significant difference in the wave spectrum occurred for the frequencies close to 0.1 Hz. Unfortunately no wave spectrum from buoy were available for analysis, and it was not possible to further study the performance of SWAN in different frequency bands.

3.6. Comparison with remote sensing data

Another available source of measurements to validate the conclusion of previous section was significant wave height data derived from SAR images. Although the reported error for SAR data is on the order of few cm (e.g. Dinardo et al., 2014; Wright et al., 1999) which is usually much higher than buoy data (less than 0.5% of measured value (Datawell, 2006), the spatial coverage of satellite-derived wave height provided a unique opportunity to evaluate the model performance for the open ocean. The statistical parameters presented in Fig. 7 shows that unlike at buoy location, the JAN and KOM formulation were more successful than WST formulation when compared with 2050 SAR data points from the model domain. These apparent discrepancies with different data sets emphasize the importance of having multiple *in situ* measurements for skill assessment of a wave models. Moreover using WAVEWATCH-III data as boundary condition for model run with WST formulation significantly improved the performance of the model. Similar to Section 3.5, using ECMWF wind data worsened the performance of the wave model compared to Grow-Fine wind data.

4. Summary and conclusion

The energy transfer from wind, quadruplet nonlinear wave interaction, and white capping dissipation are three main mechanisms controlling the wave growth and decay in deep waters. Among these three source and sink mechanisms, the white capping dissipation is the least understood term. Several formulations have been proposed for this deep water dissipation mechanism during the last two decades to improve the performance of the wave model; especially in terms of bulk wave parameters such as significant wave height, peak period and mean wave period. In this paper, third generation wave model, SWAN was implemented for

Table 3
Statistics describing the performance of KOM, JAN and WST formulations used in SWAN simulations for different time periods of simulations.

Time period		March 2002			May 2002			Aug–Sep 2003		
Parameter		KOM	JAN	WST	KOM	JAN	WST	KOM	JAN	WST
Bias	H_s (m)	0.26	0.27	0.22	0.25	0.25	0.17	0.18	0.18	0.09
	T_p (s)	−0.76	−0.94	−0.64	−1.07	−1.3	−1.0	−0.62	−0.66	−0.63
RMSE (m/s)	H_s (m)	0.39	0.40	0.37	0.4	0.41	0.35	0.41	0.42	0.37
	T_p (s)	2.7	2.72	2.71	2.45	2.67	2.4	1.82	1.86	1.81
r	H_s (m)	0.9	0.9	0.89	0.77	0.76	0.76	0.83	0.83	0.84
	T_p (s)	0.37	0.33	0.38	0.48	0.44	0.50	0.65	0.64	0.66
d	H_s (m)	0.89	0.89	0.90	0.79	0.79	0.82	0.89	0.89	0.91
	T_p (s)	0.60	0.54	0.63	0.60	0.55	0.61	0.78	0.77	0.78

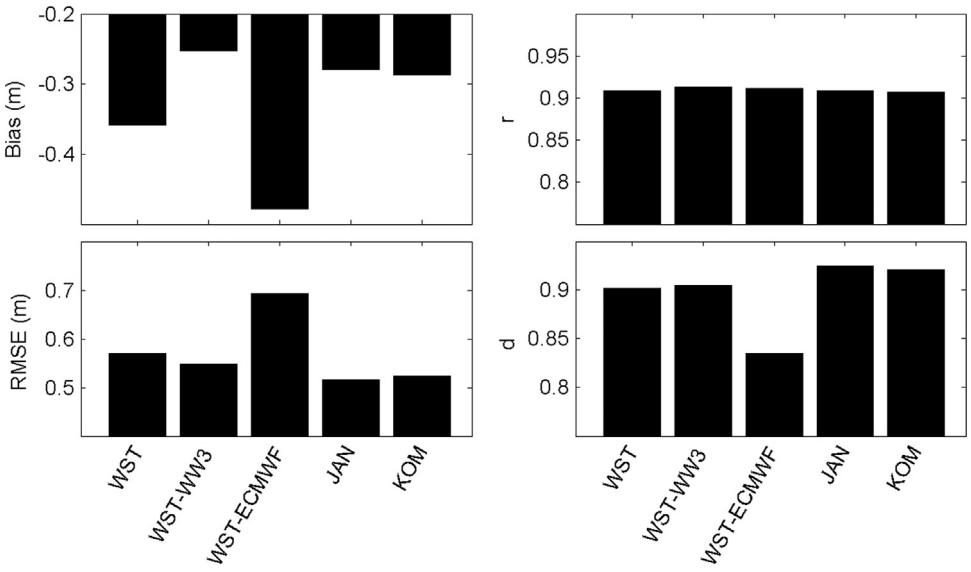

Fig. 7. Comparison of model performance using different configurations with SAR wave height during August–September 2003.

the South Atlantic Ocean near the Brazilian coast, to evaluate different wind and wave data sets in simulating wave climate of the region. Moreover, three packages for addressing white capping and energy transfer from wind to wave were statistically compared for their efficiency in simulating waves under different wind and weather conditions. Uncertainties associated with using different formulations and various wind and wave forcing were quantified from model simulations conducted for several months in 2002 and 2003. Simulation periods were carefully chosen to represent diverse wind and wave climate in the South Atlantic Ocean. It was shown that wave model results using nonlinear saturation-based white capping term presented by (van der Westhuysen et al., 2007) outperformed both WAM cycle 4 and modified WAM cycle 3 formulations when compared with buoy data.

Several statistical indices were used to describe performance of different model configurations, to avoid misinterpretations and over simplifications. A brief explanation was presented to describe each of skill-assessment parameters used in this study and potential pitfalls if we were to consider only a single parameter.

Also, significant wave height data extracted from Synthetic Aperture Radars (SAR) were employed for validation of model outputs. The remote sensing data were available along different tracks of satellites during the time periods of simulations. Unlike the excellent comparisons at buoy location using (van der Westhuysen et al., 2007) formulation, both WAM formulations worked better for saturation-based white capping term for remote sensing wave data. Note that remote sensing data were coming from deeper water depths than inshore buoy location, and the apparent discrepancy in model comparison might be related to varying performance of white capping formulations in different water depths.

The model sensitivity to two different available wind dataset and boundary wave conditions was also discussed. The wind data from satellite altimetry were used to decide which wind dataset were more realistic. It was shown that Grow-fine wind data provided by Ocean Weather Inc. were in better agreement with available measured wind data from the region. Also they were more successful in reproducing significant wave height at buoy and satellite tracks. However, using the available wave data, it was not possible to decide definitively on the best wave boundary condition data. The use of boundary conditions from Grow-Fine dataset outperformed WAVEWATCH-III data in reproducing bulk wave parameters at buoy location near to the coast. In contrast, the boundary conditions from WAVEWATCH-III simulations resulted in better wave outputs when compared with remote sensing data. Measured wave spectrum was required to further evaluate the performance of model using these two datasets.

The uncertainties in grid size and model time step were addressed using sensitivity analysis. It was shown that the selected time step and grid sizes did not affect the numerical solution of wave action conservation equation in the deep water and inner continental shelf. Also, other uncertainties in source terms and model settings were discussed briefly. The study also demonstrated the efficacy of using SAR wave data for model validation and skill assessment for remote South Atlantic Ocean, where *in situ* wave measurements are very limited.

Acknowledgments

Part of wind and wave data used in this study was provided by Ocean weather Inc. Dr. Andrew Cox is acknowledged for providing the wind and wave data for the study area. The authors thank Dr Elói Melo Filho (Engenharia Oceânica/FURG) for providing the wave data from the Southern Brazil coast.

Appendix A. Supplementary material

Supplementary data associated with this article can be found in the online version at http://dx.doi.org/10.1016/j.cageo.2015.09.025.

References

Aquaveo, 2010. Surface Water Modeling System (SMS) ⟨http://www.aquaveo.com/sms⟩.

Ardhuin, F., Rogers, E., Babanin, A.V., Filipot, J.-F., Magne, R., Roland, A., Van Der Westhuysen, A., Queffeulou, P., Lefevre, J.-M., Aouf, L., 2010. Semiempirical dissipation source functions for ocean waves. Part I: definition, calibration, and validation. J. Phys. Oceanogr. 40, 1917–1941.

Cavaleri, L., Alves, J.-H., Ardhuin, F., Babanin, A., Banner, M., Belibassakis, K., Benoit, M., Donelan, M., Groeneweg, J., Herbers, T., 2007. Wave modelling–the state of the art. Prog. Oceanogr. 75, 603–674.

Cavaleri, L., Rizzoli, P.M., 1981. Wind wave prediction in shallow water: theory and applications. J. Geophys. Res.: Oceans (1978–2012) 86, 10961–10973.

Chalikov, D., 1995. The parameterization of the wave boundary layer. J. Phys. Oceanogr. 25, 1333–1349.

Datawell, B., 2006. Datawell Waverider reference manual. Datawell, BV, Zumerlustraat 4, 2012.
Dinardo, S., Benveniste, J., Fenoglio-Marc, L., Scharroo, R., 2014. Validation of Open-Sea CRYOSAT-2 Data in SAR Mode in the German Bight, 40th COSPAR Scientific Assembly Held 2–10 August 2014, in Moscow, Russia, Abstract A2 1-32-14, p. 710.
Eldeberky, Y., 1997. Nonlinear transformation of wave spectra in the nearshore zone. Oceanographic Literature Review 44.
Hanson, J.L., Tracy, B.A., Tolman, H.L., Scott, R.D., 2009. Pacific hindcast performance of three numerical wave models. J. Atmos. Ocean. Technol. 26, 1614–1633.
Hasselmann, K., 1974. On the spectral dissipation of ocean waves due to white capping. Bound.-Layer Meteorol. 6, 107–127.
Hasselmann, K., Barnett, T., Bouws, E., Carlson, H., Cartwright, D., Enke, K., Ewing, J., Gienapp, H., Hasselmann, D., Kruseman, P., 1973. Measurements of wind-wave growth and swell decay during the Joint North Sea Wave Project . (JONSWAP).
Hasselmann, S., Hasselmann, K., 1985. Computations and parameterizations of the nonlinear energy transfer in a gravity-wave spectrum. Part I: a new method for efficient computations of the exact nonlinear transfer integral. J. Phys. Oceanogr. 15, 1369–1377.
Hasselmann, S., Hasselmann, K., Allender, J., Barnett, T., 1985. Computations and parameterizations of the nonlinear energy transfer in a gravity-wave specturm. Part II: parameterizations of the nonlinear energy transfer for application in wave models. J. Phys. Oceanogr. 15, 1378–1391.
Hwang, P.A., Ocampo-Torres, F.J., García-Nava, H., 2012. Wind sea and swell separation of 1D wave spectrum by a spectrum integration method*. J. Atmos. Ocean. Technol. 29, 116–128.
Janssen, P.A., 1991. Quasi-linear theory of wind-wave generation applied to wave forecasting. J. Phys. Oceanogr. 21, 1631–1642.
Janssen, P.A., 2008. Progress in ocean wave forecasting. J. Comput. Phys. 227, 3572–3594.
Komen, G., Hasselmann, K., Hasselmann, K., 1984. On the existence of a fully developed wind-sea spectrum. J. Phys. Oceanogr. 14, 1271–1285.
Komen, G.J., Cavaleri, L., Donelan, M., Hasselmann, K., Hasselmann, S., Janssen, P., 1996. Dynamics and Modelling of Ocean Waves. Cambridge University Press.
Kumar, R., Sarkar, A., Aggarwal, V., Bhatt, V., Bhaskaran, P., Dube, S., 2000. Ocean wave model: sensitivity experiments. In: Proceedings of the 5th International Conference PORSEC, pp. 621–627.
Rogers, W.E., Hwang, P.A., Wang, D.W., 2003. Investigation of wave growth and decay in the SWAN Model: three regional-scale applications*. J. Phys. Oceanogr. 33, 366–389.
Siadatmousavi, S., Jose, F., Stone, G., 2009. Simulating hurricane Gustav and Ike wave fields along the Louisiana innershelf: implementation of an unstructured third-generation wave model. SWAN. Proc. Oceans.
Siadatmousavi, S.M., Jose, F., Stone, G., 2011. Evaluation of two WAM white capping parameterizations using parallel unstructured SWAN with application to the Northern Gulf of Mexico, USA. Appl. Ocean Res. 33, 23–30.
Siadatmousavi, S.M., Jose, F., Stone, G., 2012. On the importance of high frequency tail in third generation wave models. Coast. Eng. 60, 248–260.
Snyder, R., Dobson, F., Elliott, J., Long, R., 1981. Array measurements of atmospheric pressure fluctuations above surface gravity waves. J. Fluid Mech. 102, 1–59.
SWAN TEAM, 2014. Swan User Manual version 41.01. Department of Civil Engineering and Geosciences. Delft university of Technology, Delft, The Netherlands.
Tolman, H.L., 2002. User manual and system documentation of {WAVEWATCH-III} version 2.22.
Tolman, H.L., Chalikov, D., 1996. Source terms in a third-generation wind wave model. J. Phys. Oceanogr. 26, 2497–2518.
van der Westhuysen, A.J., Zijlema, M., Battjes, J.A., 2007. Nonlinear saturation-based whitecapping dissipation in SWAN for deep and shallow water. Coast. Eng. 54, 151–170.
van Vledder, G.P., 2006. The WRT method for the computation of non-linear four-wave interactions in discrete spectral wave models. Coast. Eng. 53, 223–242.
Willmott, C.J., 1982. Some comments on the evaluation of model performance. Bull. Am. Meteorol. Soc. 63, 1309–1313.
Wright, J., Colling, A., Park, D., 1999. Waves, Tides, and Shallow-water Processes. Gulf Professional Publishing.
Yan, L., 1987. An improved wind input source term for third generation ocean wave modelling. KNMI.
Young, I.R., Babanin, A.V., 2006. Spectral distribution of energy dissipation of wind-generated waves due to dominant wave breaking. J. Phys. Oceanogr. 36, 376–394.
Zijlema, M., van Vledder, G.P., Holthuijsen, L., 2012. Bottom friction and wind drag for wave models. Coast. Eng. 65, 19–26.